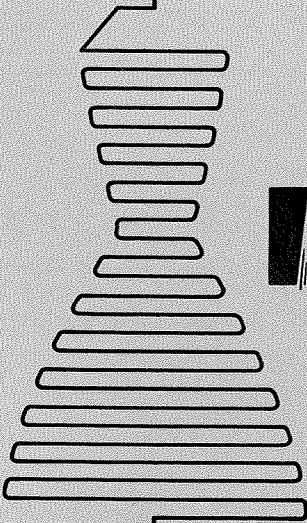


N 70 11 06 4

NASA CR 106715

R-7986

FINAL REPORT
INVESTIGATION OF POSITIVE
TYPE SHAFT SEALS



ROCKETDYNE

A DIVISION OF NORTH AMERICAN ROCKWELL CORPORATION

**CASE FILE
COPY**



Rocketdyne
North American Rockwell

6633 Canoga Avenue,
Canoga Park, California 91304

R-7986

FINAL REPORT
INVESTIGATION OF POSITIVE
TYPE SHAFT SEALS

NAS8-11325
G.O. 08624

Prepared for
National Aeronautics and Space Administration
George C. Marshall Space Flight Center
Astronautics Laboratory
Marshall Space Flight Center, Alabama, 35812

PREPARED BY

Rocketdyne Engineering
Canoga Park, California

APPROVED BY

J. O. Pfouts
Supervisor, Turbomachinery, Mechanical Elements

NO. OF PAGES 58 & viii

REVISIONS

DATE 14 November 1969

DATE	REV. BY	PAGES AFFECTED	REMARKS

FOREWORD

Rocketdyne, a Division of North American Rockwell Corporation, has prepared this report under National Aeronautics and Space Administration Contract NAS8-11325, G.O. 08624. This report covers the period from 1 September 1968, through 31 October 1969. Previous work from June 1964 through 1 September 1968 is covered by interim reports; R-6499 dated 18 April 1966, R-6811 dated November 1966, and R-6811-1 dated 25 September 1968.

ABSTRACT

The effect on seal leakage of surface finish, face load, leakage pressure, temperature, and sealed fluid were investigated. The fluids were gaseous helium, liquid hydrogen, and water. Results of a test program conducted for the investigation are presented, and a literature survey is included.

CONTENTS

Foreword	iii
Abstract	iii
Introduction	1
Task I	1
Task II	1
Task III	1
Task IV	2
Program Discussion	2
Seal Tester Design	3
Test Procedure and Apparatus	6
Instrumentation	6
Leakage Flow Analysis	6
Test Results and Discussion	13
Conclusions	23
<u>Appendix A</u>	
Flow Theory	25
<u>Appendix B</u>	
Flow Regime Method	29
<u>Appendix C</u>	
Literature Survey	31
<u>References</u>	33
<u>Bibliography</u>	35
<u>Appendix D</u>	
Distribution List for Final Report	49

ILLUSTRATIONS

1. Face Seal Static Leakage Tester	4
2. Seal Configurations	5
3. Static Seal Tester Test Setup	7
4. Flow Regimes	9
5. Leakage Parameter Dependency on Seal Load and ΔP for a 10-inch Circumference Carbon Static Seal with 8μ inch rms Surface Finish	14
6. Leakage Parameter Dependency on Seal Load and ΔP for a 10-inch Circumference Carbon Static Seal with 100μ inch rms Surface Finish	15
7. Correlation Between Ambient GHe and LH ₂ Seal Leakage	17
8. Correlations Between Ambient GHe and LH ₂ Seal Leakage	18
9. Leakage Parameter Dependence on Leaking Fluid for the J-2 Primary Fuel Seal	20
10. Leakage Parameter Dependency on Seal Surface Finish	21

INTRODUCTION

The current method employed to determine the turbopump shaft seal leakage during static conditions in-flight is to flow gaseous helium (GHe) during static ground testing and predict from the results what the static flight leakage will be. Recent experience with production turbopumps for pumping liquid hydrogen (LH₂) has indicated the lack of sufficient knowledge to extrapolate from the leakage data for GHe to that of LH₂. The relationships that exist between the parameters that govern static seal leakage are not completely understood, nor are all the flow governing parameters known.

A program was initiated to investigate the problem of flow correlation and flow predictability. The objectives of the program were: (1) to establish the relationships between GHe and LH₂ static leakage, (2) to evaluate methods of improving the technique of predicting seal leakage, and (3) to determine the causes of face seal static leakage.

The program was divided into four tasks. These are:

TASK I

Conduct a comprehensive literature survey of static leakage investigations that have been conducted with cryogens and dynamic shaft seals.

TASK II

Analyze the feasibility of various testing methods to improve the technique of evaluating the causes of and predicting seal leakage prior to the start of actual testing. The use of a transparent sealing surface will be considered for viewing the leakage during testing.

TASK III

Evaluate the effect of pressure, face loading, surface finish, surface flatness, and other factors contributing to leakage. The seal model shall be rigid enough to eliminate the distortions suspected in actual seals.

TASK IV

Test and observe actual seals of J-2 and similar designs to determine leakage correlation and the effects of pressure, temperature, and design configuration with methods of visually observing leakage during testing being considered.

PROGRAM DISCUSSION

The literature survey was initiated at the start of the program and continued through most of the other activities. The result of the survey is included in Appendix C. The feasibility of various methods of testing was evaluated, based on a substantial portion of the material from the literature survey. This evaluation indicated the difficulty encountered in the determination of the flow path geometry. The method chosen was to separate the leakage parameters during testing, study each individually, and determine the geometry parameter by flow theory. This was accomplished by flowing various fluids through the test seals and solving the flow theory equation for the geometry terms using the test data for the various fluids. This accomplishes two things: it allows the separation of the leakage parameter that describes the characteristic geometry, and gives a reference for correlation. When fluids with different physical properties are used and parameters such as pressure, load, temperature, and surface finish are held constant, the parameter describing geometry must also be constant if the correct flow theory is used.

Ambient temperature GHe and LH₂ were used because one of the program objectives was to correlate the flow from one fluid to the other. Gaseous helium at -400 F was used to determine the temperature influence between it and the ambient GHe. Water was used to give a reference for the LH₂ data because it was thought the LH₂ would change to a two-phase fluid when passing through the seal, and the H₂O would remain a liquid and therefore could be used to correlate with the LH₂.

SEAL TESTER DESIGN

The tester design chosen for the program is shown in Fig. 1. The features of the tester include a quartz optical flat mating ring, which was used to indicate parallelism during buildup and for viewing the leakage flow during testing. An alternate steel mating ring was also available. The model carbon seal support was constructed of Invar in an effort to reduce the amount of thermal distortion of the carbon seals to a minimum. Also, the model seals are fastened to the Invar sufficiently far removed from the sealing nose to further reduce the amount of thermal distortion. The deformation caused by the fasteners would decrease with distance. Therefore, the greater the distance between the fastener and sealing surface, the smaller the distortion. A comparison between the model and J-2 seals is shown in Fig. 2.

The body assembly contains an inner and outer cavity. The cavity is incorporated to allow flowing GHe at the LH_2 temperature. This is accomplished by flowing LH_2 in the outer cavity and in the cavity above the mating ring, and flowing GHe in the tube in the outer cavity, which acts as a heat exchanger and chills the GHe before it flows into the inner cavity.

The seal load is varied by the pneumatic cylinder located below the load cell. The location of the bellows allowed self-aligning of the seal. However, because the bellows MED (mean effected diameter) was affected by the varying pressure and the differences in the diameters of the seal and bellows, a calibration was therefore required prior to testing to establish the total load on the seal.

The pneumatic cylinder was of commercial design with a 1.125-inch bore. The load cell was 0- to 100-pound Baldwin.

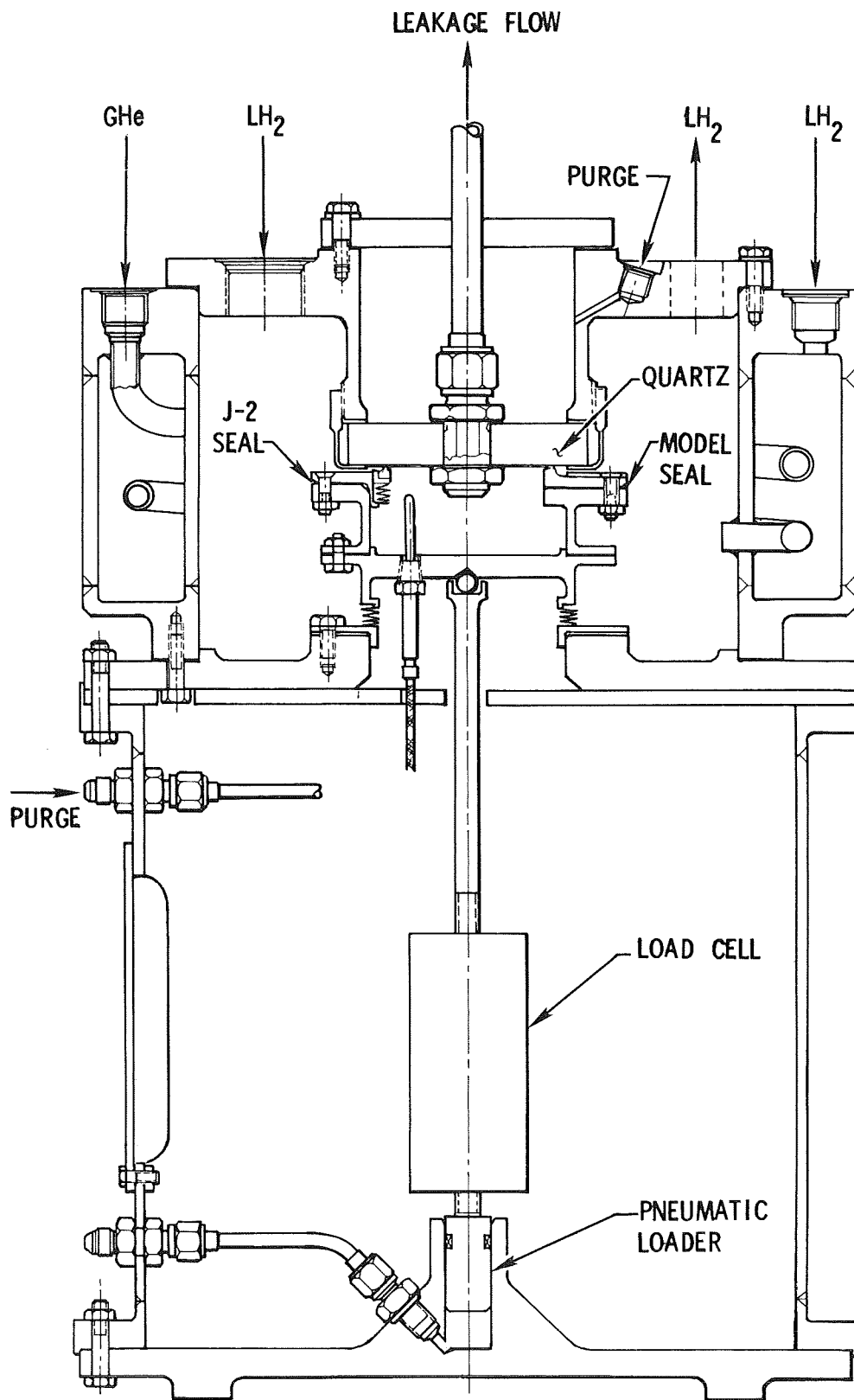


Figure 1. Face Seal Static Leakage Tester

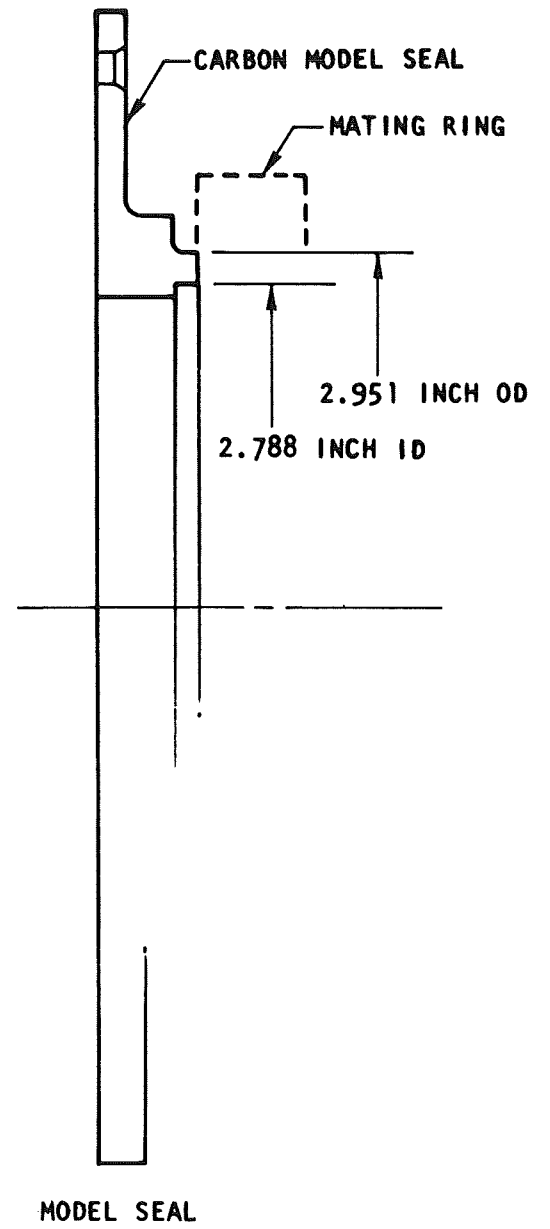
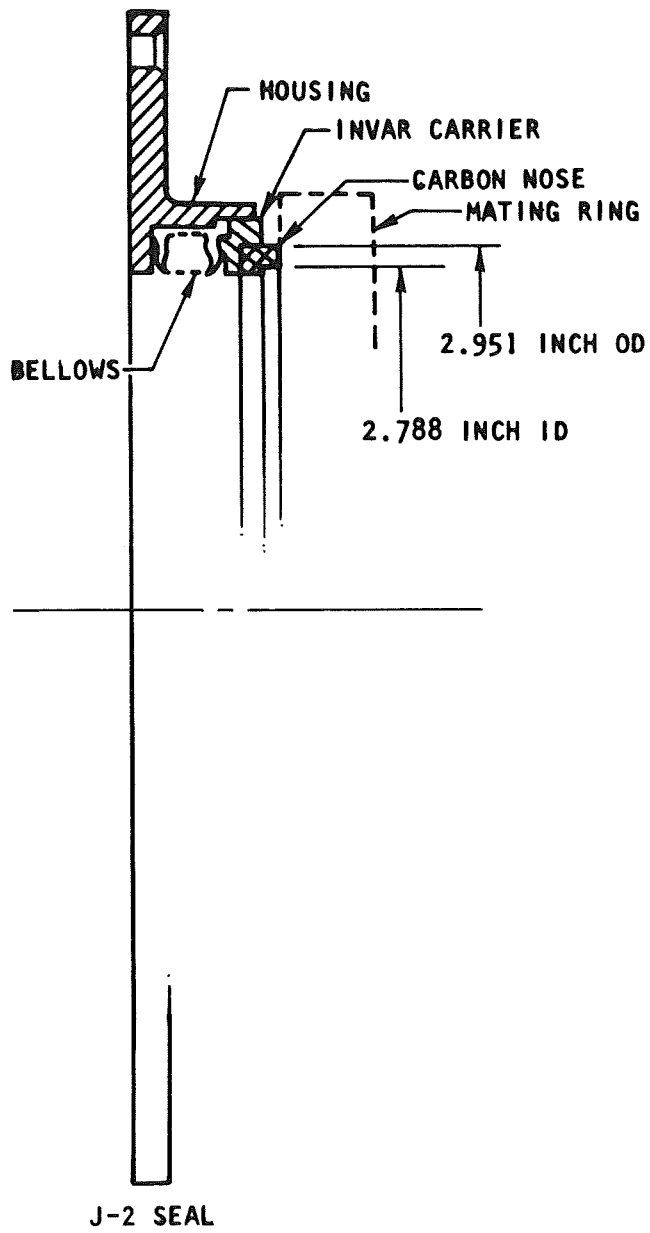


Figure 2. Seal Configurations

TEST PROCEDURE AND APPARATUS

The static seal tester is shown installed in the facility in Fig. 3. Also shown is some of the facility plumbing and instrumentation. The sequence in which the test fluids were used was 70 F GHe, -400 F GHe, LH₂, then H₂O. With each of these fluids the leakage pressure was set, and the seal nose load stepped to give a seal apparent stress of 20, 40, 60, 80, and 100 psi. The leakage pressure was increased to the next higher value and the load was increased in steps again. The leakage pressures were 13, 26, 39, 52, and 65 psig.

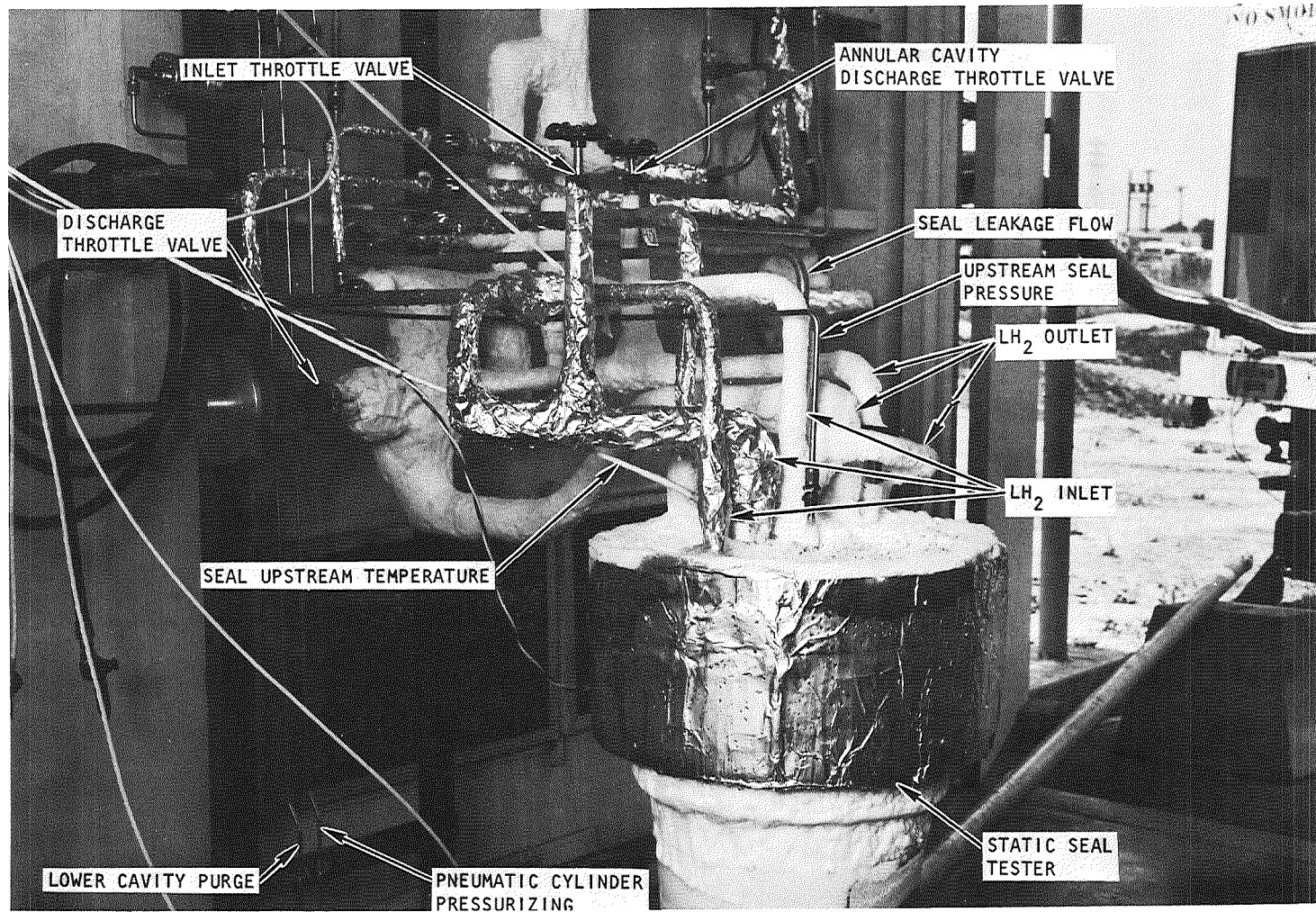
INSTRUMENTATION

The fluid state both up- and downstream of the test seal was determined, in part, with Rosemount Pt temperature bulbs. The remaining parameter, pressure, was measured with Taber transducers. Seal leakage flow was measured by H₂O displacement from a beaker with a capacity of 4800 cc.

The seal face load was measured with a 0- to 100-pound Baldwin load cell.

LEAKAGE FLOW ANALYSIS

Fluid flowing through the sealing face of a seal is described by various theories. The flow regime that exists is determined by either Mach number, Reynolds number, or molecular mean free path length. The lower limit of flow is in the molecular regime. The criterion used to indicate the existence of this regime is to compare the leakage clearance to the molecular mean free path length. The mean free path can be obtained from texts such as Ref. 1. When the mean free path length is equal to or greater than the clearance, the flow is molecular. As the leakage gap is increased, relative to the mean free path, the flow enters the transient region. This region is a combination of molecular and laminar. The regime exists until the clearance is about two orders of magnitude greater than the mean free path. Molecular flow is brought about when collisions between the molecules and the channel walls are an appreciable percentage of the total molecular collisions. A more detailed explanation can be found in Ref. 2.



1ZC65-6/27/69-S1C

Figure 3. Static Seal Tester Test Setup

Increasing the leakage clearance to the point where molecular collisions with the wall are no longer a sizable percentage of the total number will cause the flow to be laminar. The upper boundary of laminar flow is defined by a given value of Reynolds number, which in this case is about 500. By increasing the Reynolds number above this point sufficiently the beginning of the turbulent flow range will be encountered. The flow regimes above this will not be considered here. The various flow regimes can be thought of as being brought about, other things being equal, by changing the leakage clearances. Flow regimes above turbulent would require clearances much larger than encountered in face seals. Average clearances on the order of 10^{-5} to 10^{-6} inches were expected, and were confirmed by test results. The seal clearance is caused by surface asperities. Waviness of relatively long wave length as compared to the asperities could also be a factor. Surface finish measurements rarely indicate waviness. The flow regimes are shown diagrammatically in Fig. 4.

The Reynolds number based on the average flow area for the various seals and the fluid properties for the various fluids can be used to locate the relative position of the flow regimes for the various test fluids. During this program, flow measurements were made for a range of pressures at each of four fluid conditions. On the basis of these measurements at 60 psi across the seal the Reynolds numbers are:

<u>Fluid</u>	<u>Re</u>
70 F GHe	3
LH ₂	34
H ₂ O	74
-400 F GHe	104

These Reynolds numbers are sufficiently low that their usual meaning may not hold. A second method of locating the flow regimes for the various fluids is to calculate the mean free path and compare this to the "channel" dimension.

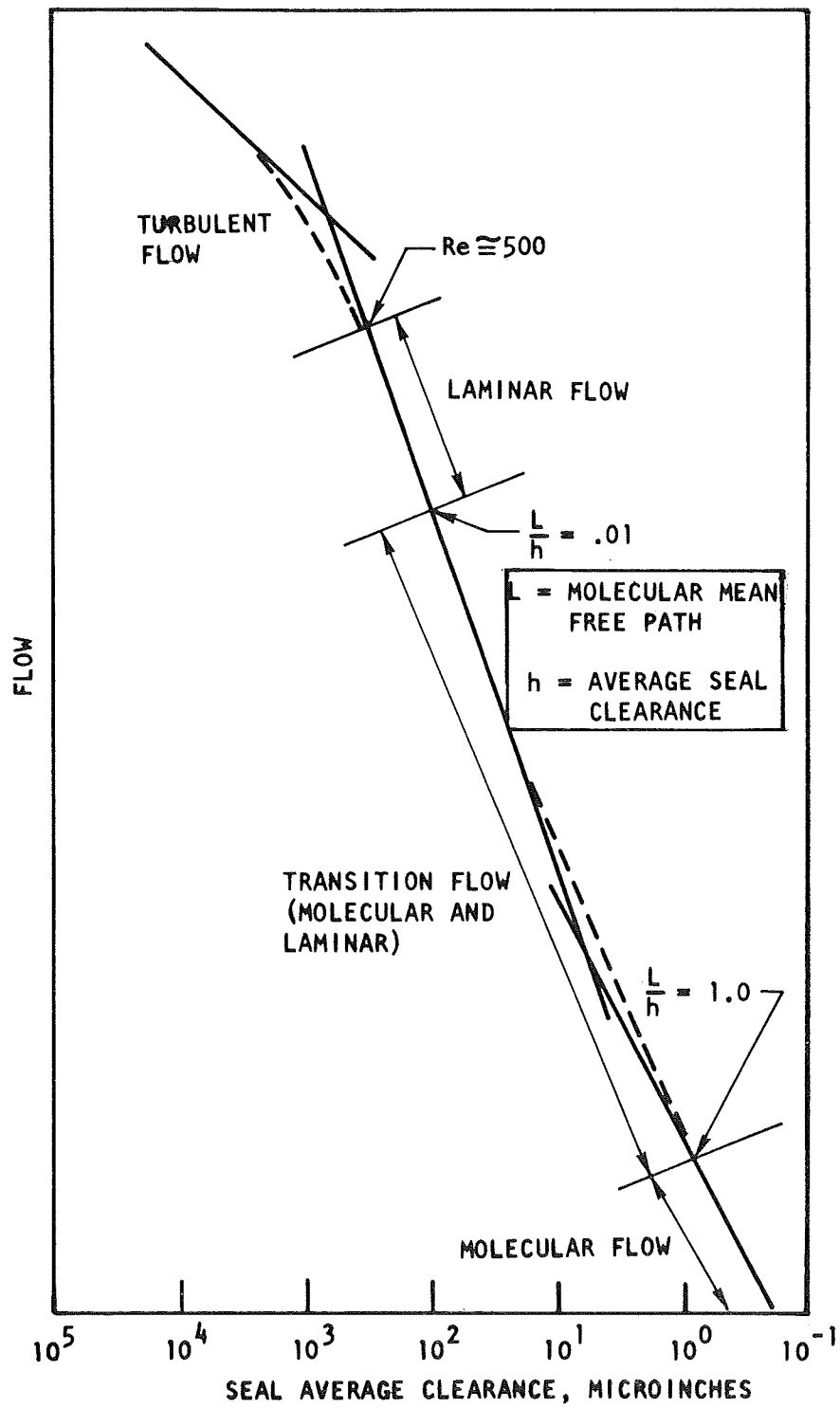


Figure 4. Flow Regimes

$$\text{Mean free path} = L = \frac{1}{\pi n \sigma^2}$$

where

$$\sigma^2 = \frac{mc}{3\pi\mu} \quad \text{and} \quad c = \sqrt{\frac{3kT}{m}}$$

k is equal to the universal gas constant divided by Avogadro's number.
T is the temperature and m is the molecular mass.

At standard conditions and GHe:

$$\begin{aligned} n &= 3 \times 10^{19} \text{ atoms/cm}^3 \\ k &= 1.37 \times 10^{-16} \text{ ergs/atom K} \\ \mu &= 1.92 \times 10^{-4} \text{ gm/cm sec} \end{aligned}$$

$$\text{for GHe } m = 4 \times 1.66 \times 10^{-24} \text{ gm}$$

at -400 F and GHe

$$\begin{aligned} n &= 10^{21} \text{ atoms/cm}^3 \\ \mu &= 4.14 \times 10^{-5} \text{ gm/cm sec} \end{aligned}$$

at -423 F and LH₂

$$\begin{aligned} n &= 142 \times 10^{17} \text{ atoms/cm}^3 \\ m &= 3.32 \times 10^{-24} \text{ gm} \\ \mu &= 1.23 \times 10^{-6} \text{ gm/cm sec} \end{aligned}$$

With the above conditions, the mean free paths for the respective fluids are:

<u>Fluid</u>	<u>MFP</u>	<u>Expected h</u>
70 F GHe	0.8×10^{-5} in.	10^{-5} in.
-400 GHe	1.6×10^{-7} in.	10^{-5} in.
LH ₂	0.6×10^{-8} in.	10^{-5} in.

These results are in conflict with the relative positions based on Reynolds number. However, because the Reynolds numbers are low and almost equal in magnitude, the criterion of mean free path is more descriptive in the flow range under consideration.

The flow theories used to describe the flow in the regimes of interest are developed in Appendix A.

TEST RESULTS AND DISCUSSION

Testing was conducted while flowing ambient temperature GHe, -400 F GHe, LH₂, and H₂O. These fluids were flowed through static carbon face seals at various pressures and various values of seal nose apparent stress (face loads).

The test results are presented as h/L vs load at constant pressures. This parameter is a function of seal geometry only and is not dependent on the test fluid. For this reason this parameter should correlate the data with the various fluids if a theory can be obtained that describes the flow while flowing each of the fluids. Plotting vs load will also indicate the dependence of the leakage parameter on load.

Figure 5 presents the data for the model seal with the 8 μ inch rms surface finish, and Fig. 6 presents the data for the 100 μ inch. Previous calculations indicated the ambient and -400 F GHe leakage would be in the transition flow regime. The mean free path calculation indicates the ambient GHe flow would be toward the molecular end of the transition regime, and the -400 F GHe would be toward the laminar. The same type of calculation indicated the LH₂ leakage would be either laminar or in the transition regime. However, this was based on flowing GH₂ instead of LH₂. The reason for this will be discussed later. A calculation for H₂O was not performed, because in a liquid the mean free path is sufficiently short to ensure laminar flow under the conditions encountered in this test program.

The LH₂ test results presented in Fig. 5 are based on transition flow theory because this theory correlated the data best of the various theories that were tried. This figure was generated by solving the transition flow equation for h/L using test data and plotting lines of constant pressure. During the LH₂ portion of the test program, an optical flat which allowed observation of the leakage was installed. A rather large amount of boiling

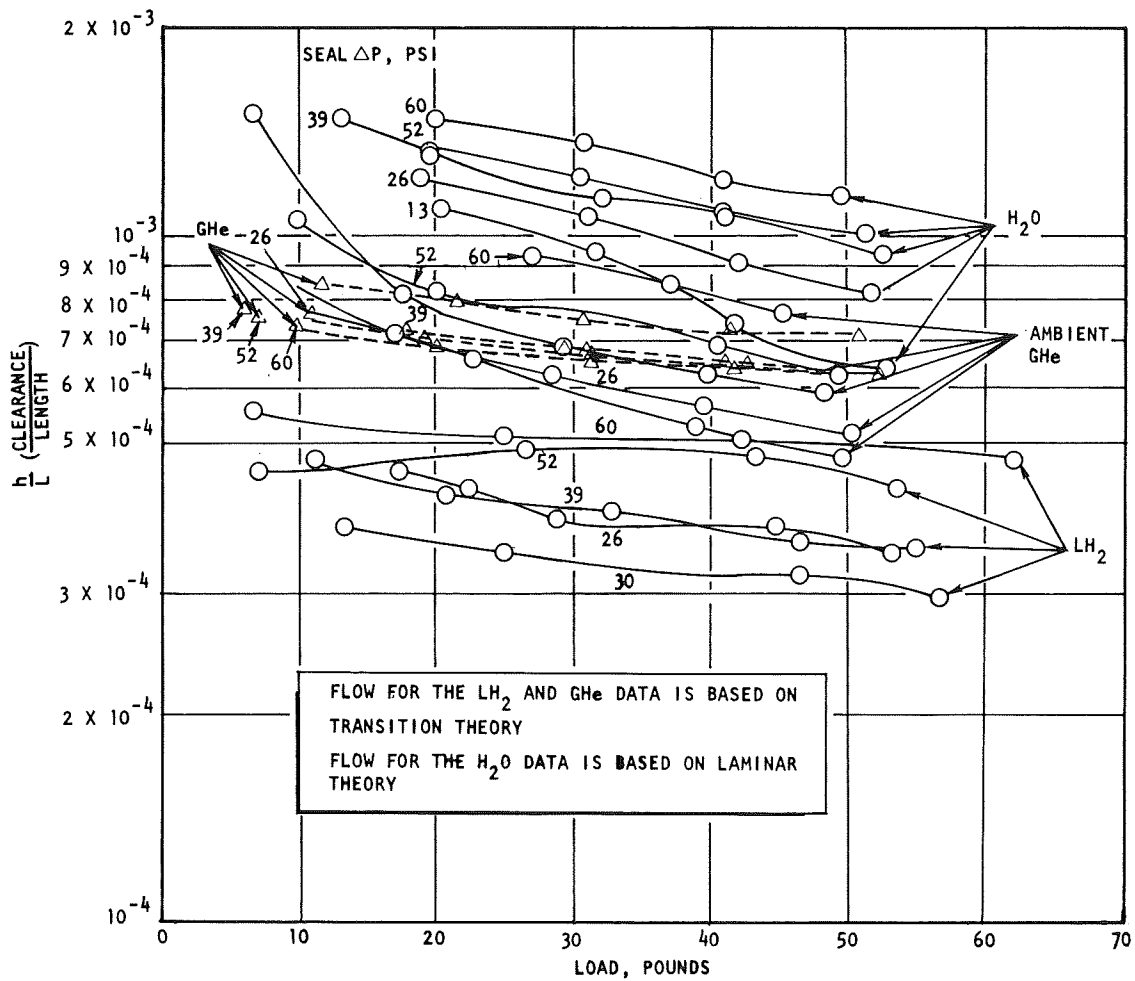


Figure 5. Leakage Parameter Dependency on Seal Load and ΔP for a 10-inch Circumference Carbon Static Seal with 8μ inch rms Surface Finish

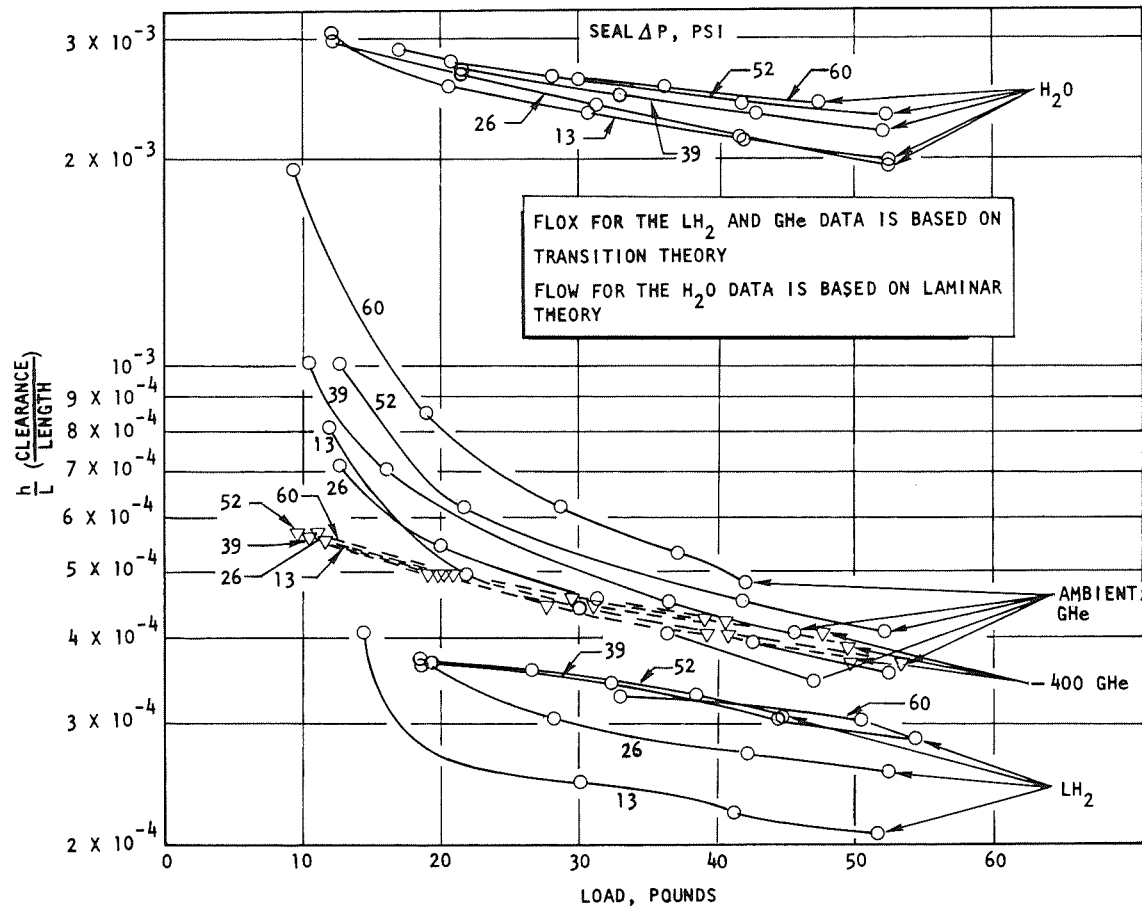


Figure 6. Leakage Parameter Dependency on Seal Load and ΔP for a 10-inch Circumference Carbon Static Seal with 100μ inch rms Surface Finish

upstream of the seal was observed, indicating the majority of leakage fluid was GH_2 and not LH_2 . If some liquid entered with the gas, it would traverse the seal with very little change in quality. This would result in a higher flow than if the flow were almost all gas. Figures 5 and 6 indicate this is not the case; therefore, it is concluded that GH_2 was flowing and not LH_2 . Taking into account the care taken to reduce heat leaks by insulating, and the observed results (that of boiling even at 60 psig), it seems very reasonable to assume that the primary J-2 fuel seal leakage during a turbopump run will also be GH_2 and not LH_2 . This may even occur during static leakage in the turbopump, that is, when the turbine is at ambient temperature.

The spread encountered in the ambient GHe , LH_2 , and H_2O data in Fig. 5 and 6 is not completely explainable. The isobars for a given fluid being separated from one another indicates the flow theory does not exactly describe the flow, possibly because of plastic deflection of the seal. By changing the order of the equation, the isobars are made to converge. This method can be used to correlate the ambient GHe and the LH_2 data and obtain a much closer correlation than is possible by following the transition flow theory. The results obtained by this method are shown for the seal with the 8 μ inch finish in Fig. 7 and for the seal with the 100 μ inch finish in Fig. 8. The isobars were made to converge by raising the flow term in the transition flow equation for the GHe data to the 0.4 power.

The above method holds for the two model seals as shown and would therefore be expected to apply to the J-2 seal. During LH_2 testing with the J-2 seal, the leakage was at least two orders of magnitude larger than with the model seals. This amount of flow could not be handled by the flowmeter. A higher capacity flowmeter was not used to measure the exact flow because the flow with GHe was about the same for the J-2 and model seals. Therefore, with the J-2 seal, the higher LH_2 leakage indicated correlation between GHe and LH_2 would not be possible with the method employed in this program, as long as the model seal data correlated. These results indicate the geometric parameter h/L is changing. To obtain a correlation

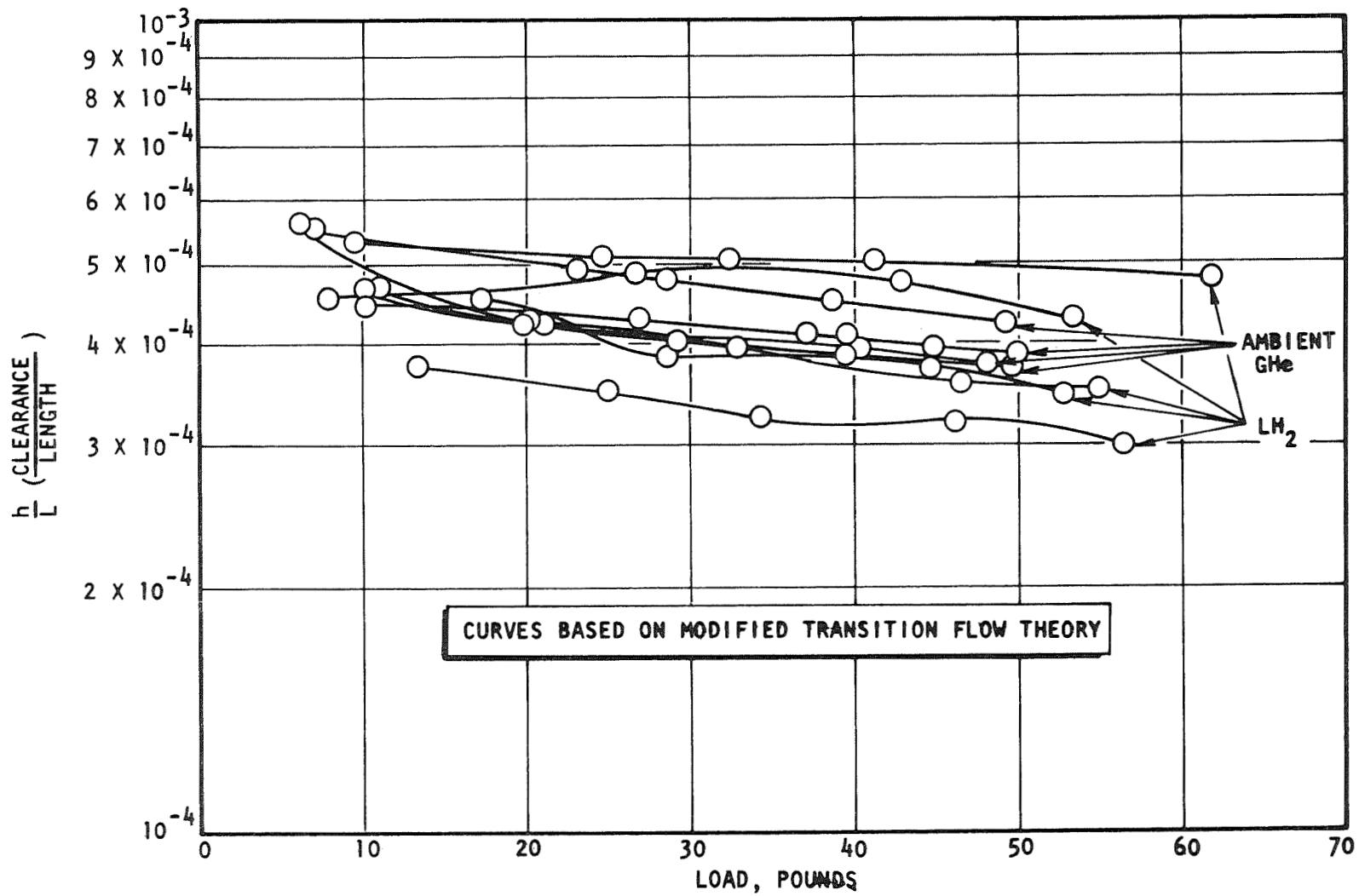


Figure 7. Correlation Between Ambient GHe and LH₂ Seal Leakage (Seal Surface Finish 8_μ inch)

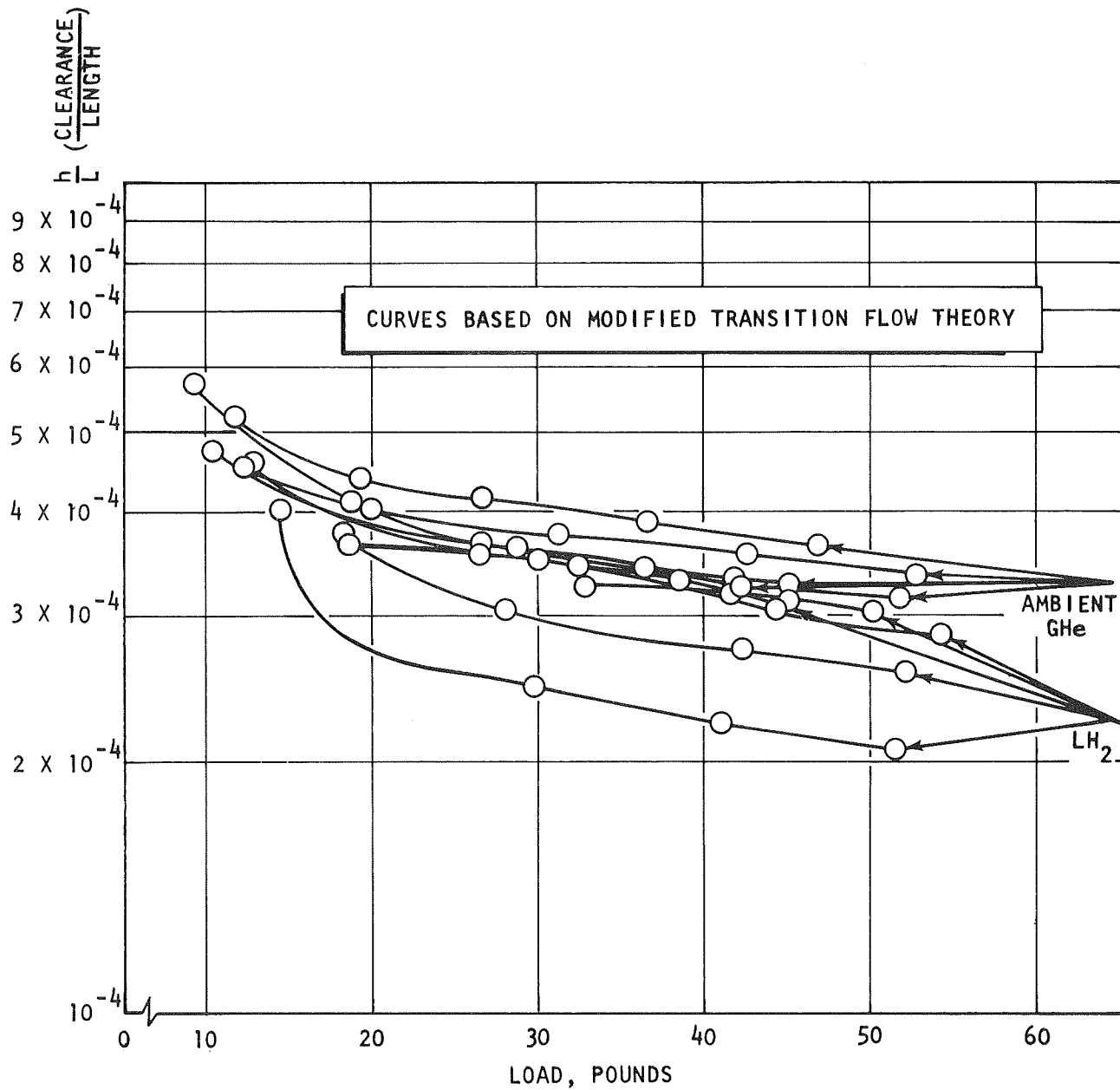


Figure 8. Correlations Between Ambient GHe and LH₂ Seal Leakage (Seal Surface Finish 100_{μ} inch)²

with this occurring would require a method such as that of statistical correlation. However, this would require a large number of data points, which is beyond the scope of this program.

This lack of correlation between the LH₂ and GHe data for the J-2 seal is thought to be caused by thermal distortion. The carbon nose is held by an Invar carrier. The carbon is lapped flat at ambient temperature, and then, when it is chilled to the LH₂ temperature, the difference in contraction between the carbon and Invar distorts the carbon, and thus the flow path. No means of predicting this distortion have been found. The model seals were designed to minimize thermal distortion, as pointed out earlier in this report. Therefore, data correlation over a large temperature difference was successful with these seals.

The H₂O data do not agree as closely as expected. Figures 5, 6, and 9 indicate the lack of agreement between the water data and the GHe and LH₂ data. The H₂O data were obtained to compare with the LH₂ data. Originally it was thought that when leaking LH₂ it would enter the seal as a liquid and change on the way through the seal to a two-phase fluid. The H₂O data would be used as a reference to correlate the LH₂ data because it remains a single phase fluid. When it was determined the LH₂ enters as a gas the H₂O data were no longer of primary interest and a better correlation was not pursued.

Returning to Fig. 7 and 8 and calculating the flow expected in LH₂ from the ambient GHe data at a load of 12 pounds results in the following: for the 8 μ inch seal, the GHe data indicate the LH₂ flow will be 0.807 cc/sec. This is the liquid flow; the gas flow would be larger by the density ratio. The test data for LH₂ indicate a flow of 1.12 cc/sec. The 100 μ inch seal gas data predict an LH₂ flow of 0.496 cc/sec as compared to the actual LH₂ test data of 0.297 cc/sec. These results indicate good correlation was achieved. However, as discussed before, the results cannot be applied to the present configuration of the J-2 primary fuel seal.

The dependence of flow on seal surface finish is presented in Fig. 10. These data are presented at a seal contact load of 12 pounds and an applied pressure of 52 psi. This curve indicates that the parameter h/L decreases

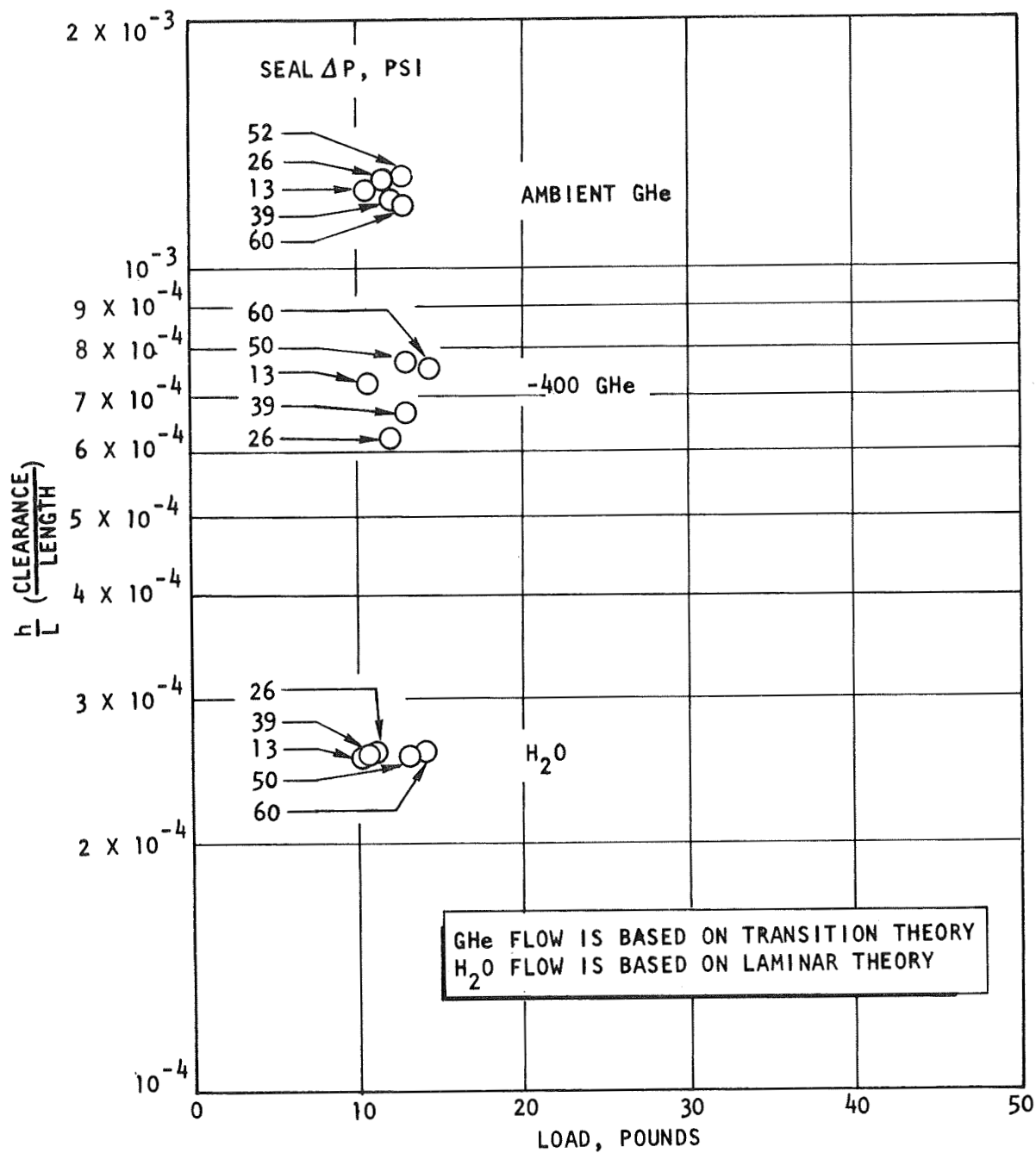


Figure 9. Leakage Parameter Dependence on Leaking Fluid for the J-2 Primary Fuel Seal

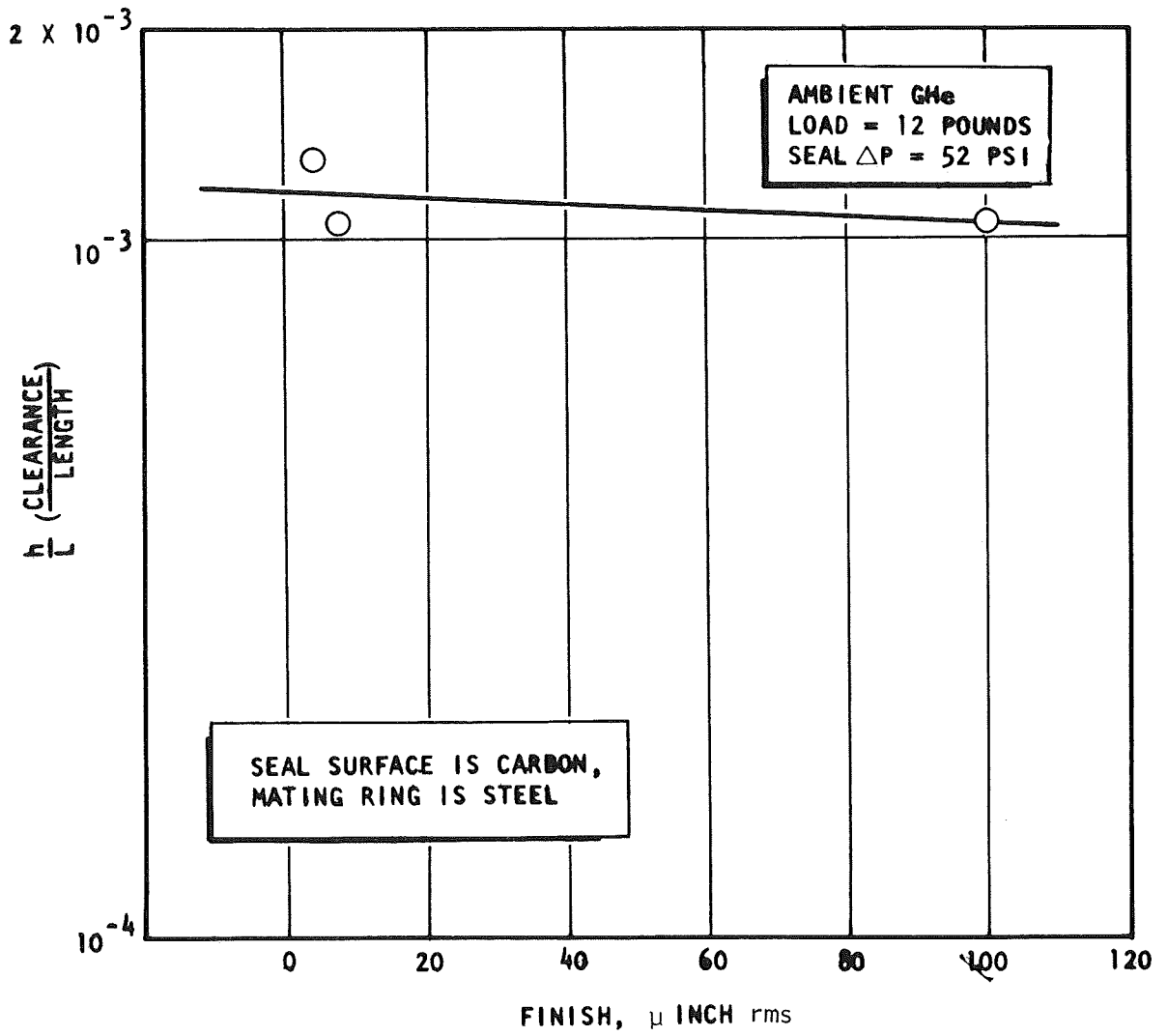


Figure 10. Leakage Parameter Dependency on Seal Surface Finish

as surface finish becomes rougher. This indicates a decrease in flow. The finish on the 100 μ inch seal tended to be concentric serrations, whereas the 4 and 8 μ inch finishes were more random. The concentric serrations would tend to seal more effectively than a random finish, and this is thought to be the reason for the results.

A quartz optical flat was used as a mating ring in an attempt to view LH_2 as it was leaking past the seal. Visual observation indicated boiling upstream of the seal was taking place but no fluid could be seen leaking through the seal. Motion pictures were also taken with a telephoto lens. The results obtained from the films were the same as the direct observations. These results, and the results based on flow theory presented earlier, indicate the leaking fluid was GHe and not LH_2 . The boiling upstream of the seal was caused by heat leaks, thus causing the leaking fluid to be a gas.

CONCLUSIONS

Based on the analytical and experimental results of this program, the following conclusions can be drawn.

Gaseous helium data were used to predict LH₂ leakage through static carbon face seals. A leakage parameter, which is a function of seal geometry only, was obtained from transition flow theory, and was used to correlate between fluids that fall in this flow regime. This theory was able to define the leakage flow even when fluid physical properties were changed.

The ability to predict LH₂ leakage from GHe test data was demonstrated. This was achieved by modifying the transition flow equation empirically. Leakage flow dependence on seal pressure drop was best defined for the -400 F GHe data and to a lesser extent for the ambient GHe and LH₂ data.

The influence of seal load on leakage was demonstrated. As would be expected, the leakage decreases as load is increased. The relationship between flow and load is nearly linear.

Leakage flow was shown to decrease as seal surface finish went from 4 μ inch rms to 100 μ inch rms, thus indicating the asperities or serrations offered more resistance to flow, possibly because they were concentric rather than being random as in the finer more lapped surface finishes.

APPENDIX A

FLOW THEORY

Molecular flow is brought about when the channel dimension is the same order as the mean free path of the gas molecule. The derivation of the equation for this regime due initially to Knudsen, Ref. 3, and was obtained from Ref. 4.

Knudsen starts with the assumption that the number of molecules striking a cm^2 of surface per second is $1/4 N\bar{c}$, where \bar{c} is the average velocity of the molecules. If there are N molecules per cm^3 , the number dN , where d is the derivative, with velocity components between c and $c + dc$ is given by the Maxwell distribution law as:

$$dN = \frac{4N}{\alpha^3 \sqrt{\pi}} c^2 e^{-\frac{c^2}{\alpha^2}} dc$$

The terms are defined in Ref. 4. Where α is the most probable speed, and e is the base of the natural log. The number of these molecules which strike 1 cm^2 of surface per second is then $1/4 c dN$. The molecules which have a component of velocity of translation w parallel to the wall on striking are absorbed and remitted equally in all directions. The momentum given the wall by these dN molecules is $1/4 c m w dN$. Since w is the component of the velocity of the gas molecules parallel to the wall, w may be written Kc where K is a constant of proportionality. This expresses w as a fractional part of c , the molecular velocity, and ascribes the Maxwell distribution to the components w in this manner. The momentum transfer is $1/4 Kc^2 w dN$. The momentum B given the wall by molecules of all velocity is therefore given by:

$$B = 1/4 NK \frac{4}{\sqrt{\pi}} m \int \frac{c^4}{\alpha^3} e^{-\frac{c^2}{\alpha^2}} dc = 1/4 NK m 3/2 \alpha^2$$

Substituting \bar{c} for α , where $\bar{c} = \frac{2\alpha}{\sqrt{\pi}}$, results in

$$B = \frac{3\pi}{32} NmKc^{-2} A\bar{c} \text{ is } \frac{\Sigma c}{N}, K\bar{c} = \Sigma \frac{Kc}{N} = \frac{\Sigma w}{N} = v.$$

This V is the geometric mean of the velocity of all molecules. It is therefore the velocity of the mass of gas down the channel, and the momentum $B = 3\pi/32 Nm\bar{c}V$, which assumes V constant across the channel.

Consider a flow channel of rectangular dimensions, dL the element of length, b the width, and A its area. In dt sec: this channel receives an amount of momentum given by $3\pi/32 Nm\bar{c}vbdLdt$. Setting $Nm = \rho$, the density of the gas, and expressing \bar{c} in terms of the pressure P , from the relation $P = \pi/8 N mc^{-2}$, the above quantity becomes $3/8 \sqrt{\pi/2} \rho \sqrt{\rho/P} vbdLdt$. If it is assumed that the wall bdL gets the whole momentum which results from the pressure drop $-(dP/dL) dL$, one obtains the relation between the momentum transfer, $-A (dP/dL) dLdt$ in the time dt due to the pressure difference across the area A , and the momentum transfer to the wall as

$$3/8 \sqrt{\frac{\pi}{2}} \rho \sqrt{\frac{P}{\rho}} vb = -A \frac{dP}{dL}$$

For G the mass flow $G = A v$, therefore:

$$G = -8/3 \sqrt{\frac{2}{\pi}} \sqrt{\frac{\rho}{P}} \frac{A^2}{b} \frac{dP}{dL}$$

If the ratio $\rho/P = \rho_1$, then

$$G = 8/3 \sqrt{\frac{2}{\pi}} \sqrt{\rho_1} \frac{A^2}{b} \frac{dP}{dL}$$

and $Q_t = G/\rho_1$, then

$$Q_t = -8/3 \sqrt{\frac{2}{\pi}} \sqrt{\frac{1}{\rho_1}} \frac{A^2}{b} \frac{dP}{dL}$$

Therefore:

$$Q_t \frac{b}{A^2} dL = -8/3 \sqrt{\frac{2}{\pi}} \sqrt{\frac{dP}{\rho_1}}$$

If the area is bh , where h is the channel height and the pressures are P_1 and P_2 ($P_1 > P_2$),

$$Q_t = \frac{1}{\sqrt{\rho_1}} \frac{(P_1 - P_2)}{3/8 \sqrt{\frac{\pi}{2}} \int \frac{b}{(bh)^2} dL}$$

Therefore

$$Q_t = 8/3 \sqrt{\frac{2}{\pi}} \frac{(P_1 - P_2) bh^2}{\sqrt{\rho_1} L}$$

Therefore, this describes the flow in the molecular flow regime. In the laminal regime the derivation is from Ref. 5. The equation for an element of fluid in static equilibrium can be written as

$$2Pby - (P-dP)2by - 2 Tbdx = 0$$

Where T is the shear defined by Newton's law of viscous flow $T = -\mu du/dy$ where u is the velocity of a particle at a distance y from the center of the passage, μ is the viscosity. Combining these two equations;

$$du = \frac{y}{\mu} dy \frac{dP}{dx}$$

Integrating with limits of $y = h/2$, $u = 0$.

$$u = \left(\frac{h^2}{8} - \frac{y^2}{2} \right) \frac{1}{\mu} \frac{dP}{dx}$$

The area of flow is $2by$ for an increment of flow dQ , therefore:

$$dQ = \frac{2by}{\mu} \left(\frac{h^2}{8} - \frac{y^2}{2} \right) \frac{dP}{dx}$$

Integrating the flow over the entire flow area, putting in limits, and adding a minus sign because dP/dx is negative in the direction of flow,

$$Q = \frac{bh^3}{12\mu} \frac{dP}{dx}$$

If $\rho gQ = w$,

$$w = - \frac{\rho gbh^3}{12\mu} \frac{dP}{dx}$$

and $\frac{P}{\rho} = RT$, the perfect gas law

$$w = - \frac{gbh^3 P}{24\mu RT} \frac{dP}{dx}$$

Integrating from P_1 to P_2 and 0 to L yields

$$w = - \frac{gbh^3}{24\mu RTL} \left(P_1^2 - P_2^2 \right)$$

The region between the molecular and laminar is known as the transition region. In this region both laminar and molecular flow effects are in operation. The method used to describe this flow regime is the direct addition of the two flow theories. The result is:

$$w = 8/3 \sqrt{\frac{2}{\pi}} \frac{bh^2 (P_1^2 - P_2^2)}{\rho L \sqrt{\rho_1}} + \frac{bh^3 (P_1^2 - P_2^2) g}{24\mu LRT\rho}$$

This resulting equation is cubic. The method employed to determine a solution is shown in Appendix B.

APPENDIX B

FLOW REGIME METHOD

CUBIC 08:14 ROCKET SEPT. 8, 1969

10 DIMENSION VIS(50), T(50), P1(50),
20&P2(50), W(50), RHO(50)
30 DATA NCNT/1/
40 DATA B/10.0/
50 DATA RR/386.2/
60 DATA EL/0.1/
70 DATA VIS/0.0465, 49*0.0/
80 DATA T/520.0, 49*0.0/
90 DATA P1/13.0, 49*0.0/
100 DATA P2/50*0.0/
110 DATA RHO/0.0215, 49*0.0/
120 DATA W/6.87, 49*0.0/
130 PI=3.1415926
140 GB= 32.174*B
150 RL=RR*EL
160 Z1=4.0/3.0*SQRT(2.0/PI)
170 C1= 2.54↑3*1728.0
180 C2= C1*32.174*3600.0*12.0
190 DO 100 I=1, NCNT
220 CC2=C2/RHO(I)
230 CC1=C1/RHO(I)
240 P1P2=(P1(I)+13.8)↑2 - (P2(I)+13.8)↑2
250 DELP = P1(I)-P2(I)
260 D1= 24.0*VIS(I)*RL*T(I)
270 D2=DELP/SQRT(RR*T(I)/32.174)
330 Y1=GB*P1P2*CC2/D1
340 P1=Z1*B/EL*D2*CC1
350 Q1=0.0
360 R1=-W(I)

```

370 P=P1/Y1
380 Q=Q1/Y1
390 R=R1/Y1
400 AA=(3.0*Q-P^2)/3.0
410 BB=(2.0*P^3-9.0*P*Q+27.0*R)/27.0
420 TEST=BB^2/4.0+AA^3/27.0
450 IF(TEST) 2, 3, 3
460 3 BIGA=(-BB/2.0+SQRT(TEST))^0.333333333
470 BIGB=(-BB/2.0-SQRT(TEST))^0.333333333
480 X1= BIGA+BIGB-P/3.0
482 PL=X1^3/EL
490 GO TO 230
500 2 COSPHI=-BB/2.0/SQRT(-AA^3/27.0)
510 X=COSPHI
520 PHI=ATAN(SQRT(1.0-X^2)/X)
530 X1=2.0*SQRT(-AA/3.0)*COS(PHI/3.0)-P/3.0
540 X2=2.0*SQRT(-AA/3.0)*COS(PHI/3.0+120.0*0.01745333)-P/3.0
550 X3=2.0*SQRT(-AA/3.0)*COS(PHI/3.0+240.0*0.01745333)-P/3.0
552 HL=X1^3/EL
560 PRINT 4, X, PHI, X1, X2, X3
570 4 FORMAT(10X, 7HCOSPHI=, F12.5/10X4HPI=, E12.5/
580&10X3HX1=, E12.5/10X3HX2=, E12.5/10X3HX3=,E12.5)
582 PRINT 7, HL
584 7 FORMAT(10X7HH**3/L=, E12.5)
600 GO TO 100
610 230 PRINT 5, X1, HL
620 5 FORMAT (10X, 2E20.7)
630 100 CONTINUE
640 END

```

READY

APPENDIX C

LITERATURE SURVEY

The purpose of the literature survey was to obtain information pertinent to the establishment of a testing method and analysis procedure with sufficient depth to satisfy the program requirement.

The sources used for the search were NASA, DDC, and TIPS. TIPS is a company-wide index that is an electronic-computer-orientated system. The inputs to this system are obtained from the vast number of sources that have any of the North American Rockwell divisions on their distribution lists. Also, there was a manual search conducted through indexes of both periodical and aperiodical literature.

The manual search was conducted through six technical indexes and the Rocketdyne library card catalog. Search dates started from the present and continued back as far as 1950 where possible. The indexes that were covered were: Aeronautical Engineering index, Aerospace Engineering index, Aerospace Engineering Review and International Aeronautical abstracts, Applied Science and Technology index, Engineering index, and the Nuclear Science abstracts.

The total number of references turned up, including those from previous searches, was about 3000. The previous searches are included for reference. The references that are most pertinent to the program are included in the bibliography along with their abstracts.

REFERENCES

1. Hirschfelder, Curtiss, and Bird: Molecular Theory of Gases and Liquids, J. Wiley and Sons, New York, 1954.
2. Duschman, S. and J. Lafferty: Scientific Foundations of Vacuum Technique, J. Wiley and Sons, New York, 1962.
3. Knudsen, M: Ann. Physik, 28, 75, 999 (1909); 35, 389 (1911).
4. Lobe, L.: Kinetic Theory of Gases, McGraw Hill, Inc., New York and London, 1934.
5. Grinnel, S.K.: "Flow of a Compressible Fluid in a Thin Passage," ASME 55-SA-13, May 1956.

BIBLIOGRAPHY

1. Hamilton, D. B., J. A. Walowit, and C. M. Allen: "A Theory of Lubrication by Microirregularities," Journal of Basic Engineering, Trans. of the A.S.M.E., Series D, Vol. 88, No.1, March 1966, pp 177-185.

This paper describes a theory of liquid lubrication applicable to parallel surfaces, such as the surfaces of a rotary-shaft face seal. The lubrication mechanism presented is based on surface microirregularities and associated film cavities. Closed-form analytical solutions are obtained giving load capacity as a function of speed, viscosity, and surface-asperity dimensions. The theoretical results agree qualitatively with load capacity determined experimentally for three asperity distributions.

2. Davies, M. G.: "The Generation of Lift by Surface Roughness in Radial Face Seals," Int. Conf. on Fluid Sealing, Paper E-4, April 17-19, 1961, B.H.R.A.

The idea is developed that large pressures of questionable origin in oil filled clearance between surfaces of radial face seals is due to hydrodynamic lubrication effects in small wedge-shaped cavities constituting surface roughness. The consequences of the theory in regard to leakage and seal design are discussed.

3. Bauer, P.: "Investigation of Leakage and Sealing Parameters," IIT Research Institute, Technical Report AFRPL-TR-65-153, August 1965.

The report documents investigations conducted to expand and refine analytical techniques for static and dynamic seals. A systematic investigation was made on those aspects of a seal pertaining to the sealing interface, structure, cavity, and related parts. Since the sealing interface was the problem area most lacking in reliable and concise information, major effort was directed toward its study. The

problem was approached both analytically and experimentally by independently studying sealing interfaces with and without gross relative motion. The parameters influencing static interfaces were identified as surface finish, applied load, contact area, and material hardness. These parameters were correlated to form design criteria suitable for use by systems designers to predict seal leakage performance. Additionally, these parameters were studied for rubber contact interfaces with wear added as the most significant parameter. The importance of wear on seal leakage was identified not as surface damage but as the effect of wear debris fragments and frictional heating. To the extent of experimentally supported information, all parameters were correlated in the form of design criteria. The output from these and other investigations produced applicable criteria and provided an insight into the relationship between parameters that can be used to optimize sealing and serve as guidelines for attaining minimum leakage. Commercial and other seals were utilized to show, by example, the design and analysis techniques leading to leakage performance predictions. The degree of success achieved was established by demonstration of experimental performance.

4. Miyakawa, Y.: "Influence of Surface Roughness on Boundary Friction," Journal of the American Society of Lubrication Engineers, May 1965.

The effects of surface roughness on boundary friction is studied under various conditions of loads, speeds, and lubricants.

As the result of experiments, it is found that the direction of polishing to the direction of sliding greatly influences the boundary friction. The friction, sliding parallel to the direction of polishing, is larger than that in the perpendicular direction. The degree of roughness has little influence upon the friction, except in the case of extremely small or large degree of roughness. The effective lubrication occurs as a result of the interruption of contact by the

surface roughness. Therefore, the most effective lubrication takes place when the sliding surface is perpendicular to the direction of polishing and the surface has an appropriate degree of roughness.

5. Dawson, P.: "Investigation of Cavitation in Lubricating Films Supporting Small Loads," Proc. Conf. On Lubrication and Wear, Paper 49, pp. 93-99, Oct. 1-3, 1957, Instn. Mech. Engrg., 1 Birdcage Walk, London, SW 1.

Bearing surfaces in the form of stationary spherical cap and a plane slider have been used to provide visual observations and pressure records of the conditions in the clearance space under full and cavitating conditions. Satisfactory correlation of the pressure records and visual records has been obtained. A departure from predictions is noted in the form of a downstream shift of the oil film rupture point.

6. Allen, C. M., J. C. Bell et al.: Rotating-Shaft Helium Seal Investigation. Battelle Memorial Inst., Columbus, Ohio, NP-11243 Contract DA-44-009-eng-3375 (71 pp.), 25 August 1959.

A research program was conducted to study positive rotating-shaft seals using helium for high-speed turbomachinery.

7. Jakobsson, B. and L. Floberg: "The Finite Journal Bearing, Considering Vaporization," Trans. of Chalmers University of Tech., No. 190, 1957, Gothenburg, Sweden, Report No. 3 from The Institute of Machine Elements.
8. Wilkinson, S. C. W.: "Mechanical Seal Design," Engineering Materials and Design, V. 5, pp. 572-576, 664-667, Aug.-Sept. 1962.

Radial face-type shaft seals. The following design features are discussed: surface finish, mechanical seal distortion, hydraulic face

distortion, heat dissipation paths, adequate cooling circulation, wetting properties, fluid pressure relative to face loading, seal balance, and solids in suspension.

9. Crego, D. F.: "Centrifugal Compressors: Seals and Sealing Systems," Petroleum Refinery, 7. 34, pp. 143-6, Jan., 1955; Petroleum Engineer, V. 28, pp. C17-22, Feb., 1956.

Straight pass labyrinth, staggered labyrinth, segmented carbon rings, and contact or mechanical seals are discussed. Three types of sealing systems, evacuation, gas injection, and fluid injection are also discussed.

10. Batch, B. A., B. A. Goldring, P. E. Winney: "An Instrument for Measuring the Main Surface Profile on Seal Faces," Journal of Scientific Instruments, Vol. 1, Series 2, 1968.

The design, construction, and performance of an instrument for measuring the surface profile of nominally flat seal-rings associated with an experimental mechanical seal are described. The device, which utilizes the principles of the aerostatic thrust bearing, is capable of measuring profiles of a few microinches amplitude superimposed on a face run-out greater by two orders of magnitude.

11. McCray, C. R.: "Radial Positive-Contact Seals," Machine Design, The Seals Book, pp. 9-14, Jan. 19, 1961.

A radial positive contact seal is a device which applies a sealing pressure to a mating cylindrical surface to retain fluids and sometimes exclude foreign matter. Rotating shaft application is most common but also applied to oscillatory or reciprocating motion.

Various types are discussed together with seal selection criteria and their significance. Attendant problems, cause and cure, is also covered.

12. Dega, R. L.: "Recent Advances in Lip Seal Technology," National Conference Industrial Hydraulics, 14 pp., 154-63, October 1960.

Presents the variables which affect seal operation, shaft, assembly, seal, lip dimension variables, diameter, pressure, eccentricities, lip material quality. Also types defects with photos. Presents data curves, temperature vs speed, hardness variation due to curing time, friction coefficients for various hardness and surface finishes, etc., and discussion.

13. Grinnel, S. K.: "Flow of a Compressible Fluid in a Thin Passage," ASME 55-SA-13, May 1957.

Pressure distribution and weight-flowrate can be predicted for laminar compressible-fluid flow in a thin passage by use of the methods presented in this paper. A simplified method can be used readily when the fluid forces due to viscous action predominate over those due to acceleration of the fluid. A more complicated trial-and-error method seems to be required for larger passages where, though the flow may be laminar, the momentum effects due to acceleration of the compressible fluid are appreciable. An experimental apparatus was used to examine the validity of the analytical work. Experimental pressure distributions agree within a maximum deviation of 10 percent with the theoretical distributions predicted by both the comprehensive and simplified theories. Experimental weight-flowrates agree within a maximum deviation of 50 percent with predictions of the simplified theory. Dimensionless plots of pressure distribution are presented with experimental curves of flowrate vs pressure ratio for various ratios of passage length L to passage height h . These plots, together with simple equations, have been prepared for direct use by the designer.

14. Denny, D. F.: "Some Measurements of Fluid Pressures Between Plane Parallel Thrust Surfaces and Special Reference to Radial Face Seals," Wear, V. 4, No. 1, pp. 64-83, 1961.
15. Nau, B. S. and D. E. Turnbull: "Some Effects of Elastic Deformation on the Characteristics of Balanced Radial Face Seals," Int. Conf. on Fluid Sealing, Paper D3 (8 pages), April 17-19, 1961, British Hydro-mechanics Research Assn., Harlow, Essex, England.

When a relatively small amount of pressure balancing is used in design of radial face seals, they are able to run with a very thin fluid film separating the faces. Test results show that with local deformations on the face, the film is capable of supporting a greater load than predicted when no deformation occurs.

16. Dawson, L. J.: Development and Design of Mechanical Seals for Centrifugal Pumps, Ingersoll-Rand, 1950.

A description of the origin and development of seals employing radial mating surfaces serves to show which features of the whole gland inherently cause the most trouble. Illustrations and designs.

17. Tao, L. N and W. Donovan: Through-Flow in Concentric and Eccentric Annuli of Fine Clearance With and Without Relative Motion of Boundaries," ASME Trans., V. 77, pp. 1291-1301, 1955.

Derives theoretical flow equations for title conditions. Certain assumptions by authors questioned in discussion by Teichmann. Experimental data, in good agreement with theoretical equation, are presented in graphical form for Reynolds' numbers up to 30,000. Thermal effects, phase change, and compressible flow are not included.

18. Huhn, D." "Theory of Fluid Sealing," Int. Conf. On Fluid Sealing, Paper D2, (8 pgs.), April 17-19, 1961.

Basic laws for leakage, wear, and power requirements are deduced from the general equation for fluid motion, for radially and axially contacting seals. Pressure forces, and their influence, as well as improvement by hydraulic balance are discussed. Shaft eccentricity, vibrations, surface conditions to power consumption, and heat development by rotating seal parts were not considered.

19. Findlay, J. A.: "Cavitation in Mechanical Face Seals," ASME, 67-WA/LUB-20.

The characteristics of mechanical face seals operating with hydrodynamic films containing gas cavities were studied. Solutions to Reynolds' equation for hydrodynamic lubrication were obtained using both the short bearing approximation and numerical iterative methods. These two methods of solution satisfy continuity of flow throughout the seal film. Leakage rates and seal hydrodynamic loads were calculated. Some computed cavity shapes are also given.

20. Gaibel, E. and F. A. Lyman: "A Theoretical Investigation of Leakage Through Rotary Shaft Seal," Report 850489, U. S. Naval Eng. Experiment Sta., Annapolis, Nov. 28, 1961.

It was shown that the effect of face waviness, non-parallelism of faces, or a notch in the seal face could be sufficient to generate a fluid film between the faces. Approximate solutions to the Reynolds' equations are derived by using perturbation methods, and comparison with previously published results shows fair agreement.

21. Summers-Smith, D. "Laboratory Investigation of the Performance of a Radial Face Seal," Int. Conf. on Fluid Sealing, Paper D1 (12 pages), April 17-19, 1961. British Hydromechanics Research Assn., Harlow, Essex, England.

The performance of a radial face seal in terms of leakage, wear, and friction torque in a rig in which the liquid pressure and contact loading of the seal face could be varied independently. Sealed water at pressures up to 50 psi. Friction and wear measurements indicate that for normal operation a fluid film (approximately 100 microinches thick) is generated between the sealing faces.

22. Nau, B. S.: Cavitation in Thin Films, The British Hydrodynamic Research Association, TN 832, Nov. 1964.
23. Bell, K. J. et al.: "Flow Through Annular Orifices," A.S.M.E., Transactions, Vol. 79, pp. 593-601, April 1957.

Coefficients for the annular orifice formed between a circular disk and a cylindrical tube are reported for twenty-one orifices having disk diameter to tube diameter ratios in the range of 0.95 to 0.996, and orifice length-to-width ratios from 0.118 to 33.3. The orifice Reynolds number range is from 2.0 to 20,000 for both tangent and concentric orientations of the disk. Comparison with previous data indicates that the results also apply to the annular orifice formed when a rod extends through a circular hole in a plate. Theoretical and semi-empirical equations are developed to predict coefficients for annular orifices.

24. Rudinger, G.: "Nonsteady Discharge of Subcritical Flow," A.S.M.E., Paper 60-WA-152 for Meeting Number 1960.

The calculation of a nonsteady flow discharging into the atmosphere, or into a large reservoir, is generally based on the assumption that the effective exit pressure is the same as if the flow were steady. In reality, however, the steady-flow boundary conditions are asymptotically approached after a disturbance produced by an incident wave, and recently published investigations provide a better approximation to these transient boundary conditions. Utilizing these results, one

can compute the rate of discharge and compare it with the rate obtained in the conventional manner. The difference between the results of the two calculations is used to define a lag error in the conventional calculations. Examples for discharges through an open end and through a sharp-edged orifice indicate that the actual transient flowrate may deviate considerably from that computed on the basis of steady-flow boundary conditions.

25. Gresham, W. A., Jr. et al.: "Review of the Literature on Two-Phase (Gas-Liquid) Fluid Flow in Pipes," Engineering Experiment Station of the Georgia Institute of Technology, WADS-TR 55-422, June 1955, Contract AF33(616)2660, AD 95752.

All available literature on the subject of two-phase (gas-liquid) fluid flow was studied and the significant literature is summarized in this report.

Gas-liquid flow can be classified into at least seven different types of flow in horizontal ducts and five types in vertical ducts. For a given combination of fluids, it is possible to roughly correlate the flow types with the flowrates.

Most of the early workers utilized friction factor-type relations in their attempts to correlate the pressure drops and flowrates. The first generalized relation was presented by Martinelli and co-workers who correlated the two-phase pressure drop with that of the liquid or gas assumed to flow alone in the duct. Most subsequent investigators have used modifications of this correlation. A few investigators have attempted to solve relations based on the continuity, energy, and momentum equations.

Abstracts of 180 references are included.

26. Vermes, G.: "Fluid Mechanics Approach to Labyrinth Seal Leakage Problem," A.S.M.E. Transactions, Series A, Journal of Engineering for Power, Vol. 83, pp. 161-9, April 1961.

The paper describes investigations of labyrinth seals carried out recently; derives new theoretical and semitheoretical formulas for computation of the leakage which agree within 5 percent with the tests for three different types of seals; off-design performance of the seals is treated theoretically and experimentally.

27. Zabriskie, W. et al.: "Labyrinth Seal Leakage Analysis," A.S.M.E., Transactions, Series D, Journal of Basic Engineering, Vol. 81, pp. 326-6, September 1959.

The leakage flow through labyrinth seals in turbomachinery has been the subject of increasing concern as refinements and advances in design are made. Accurate knowledge of seal leakage is necessary in at least three areas of design: (1) estimating the effect of seal leakage on performance; (2) regulating the leakage flow required for cooling purposes; (3) determining the thrust-bearing load which is a function of the pressure drop through the seal. This paper is concerned primarily with the fluid-flow aspect of gas leakage through labyrinth seals of the types commonly used in gas and steam turbines. This includes staggered and unstaggered seals of the axial type, which are most commonly used in turbomachinery. The attention to fluid flow considerations does not imply that material compatibility and operating problems of expansion, deformation, and rub-in are unimportant. In fact, these mechanical considerations may overrule the fluid flow considerations. For the foregoing reasons, it is desirable to be able to predict seal leakage flows, and thus this aspect of seal design has been singled out for consideration here.

28. Kearton, W. J.: "Flow of Air Through Radial Labyrinth Glands," Inst. of Mech. Engrg., Proceedings, Vol. 169, pp. 539-52, 30, 1955.

A theory for the flow of air through a radial gland has been worked out for both outward and inward flow. Expressions are derived for the pressure distribution in each kind of flow, and it is shown that the critical pressure ratio can be reached only in the final constriction. Experiments were made on a gland having a single ring and also on a 20-ring gland of the staggered type. The discharge coefficients in the latter gland were lower than those in the single-ring gland, possibly due to the different approach conditions. The observed pressure distribution in the multiring gland agreed well with the theoretical value. Finally, some experiments were made with unstaggered radial glands under various conditions. Discharge coefficients greater than unity were measured.

29. Miller, E. E. et al.: "Physical Theory for Capillary Flow Phenomena," Journal of Applied Physics, Vol. 27, pp. 324-32, 1956.

From the assumption that the microscopic behavior of the liquid in an unsaturated porous medium is controlled by the physical laws of surface tension and viscous flow, differential equations governing the microscopic flow in such a medium are deduced. No special pore-shape assumptions are required, but one topological approximation is needed; i.e., that neither isolated drops nor isolated bubbles occur. Several nonessential simplifying assumptions are used; i.e., that the microscopic properties of the medium, the character of the liquid, and the pressure of the gas are independent of position, time, and direction. The microscopic equations are obtained in a fully reduced form, permitting comparison between two media, or between two flow systems, that differ only by scaling factors.

A novel feature of this calculation is its prediction that the liquid-transmission and liquid-capacity properties of an unsaturated medium will exhibit hysteresis in their dependences upon the liquid-gas

pressure differential, ΔP . The properties of the medium depend upon the pressure history but are invariant to monotonic time-scale distortions of that history. Such time-invariant functionals have been termed by the authors hysteresis functions," symbolized by the subscript, H; e.g., $F_{H(p)}$. Although methods for measuring and describing the characteristics of specific "hysteresis functions" have not yet been developed, the general validity of this analysis can be studied experimentally by testing predictions that are contained in the reduced variables.

30. Mayer, E.. "Leakage and Wear in Mechanical Seals," Machine Design, Vol. 32, pp. 106-13, March 3, 1960.

What are the major factors causing leakage and wear in mechanical seals? Can leakage be calculated accurately? What can be done to reduce leakage and wear?

Tests on unbalanced seals for 20,000 hours, with five face material combinations, and three different fluids, have given some answers: No fluid pressure exists between seal faces, in contrast to previous theories. Leakage, wear, and friction are determined by boundary lubrication. Surface width has no influence on leakage. Physical results confirm a new theory of fluid-exchange flow. Leakage varies with the square of the distance between touching faces, and inversely with the square of the face pressure. No influence of viscosity has been noticed. Leakage is the same for all fluids, but nearly 100 times greater for external than for internal rotating seals. Results reported are not limited to mechanical seals and may also be used for oil seals, piston rings, and clutches.

31. Tolansky, S.: "Surface Microtopography," Internal Science and Technology, Vol. 9, pp. 32-9, September 1962.

Knowing the true character of the surface of materials, even down to microstructures of molecular dimensions, is becoming increasingly

important. Such information can tell how surfaces are formed, how they are distorted under various influences, and how they are destroyed. Multiple-beam interferometry is one of the most powerful tools for examining the microtopography of a surface. As presently practiced, it can magnify the vertical dimension of surface irregularities up to 500,000 times. This sensitivity means that vertical displacements as small as 5 angstroms can be detected by the interference of many light beams reflected from the surface under study with those reflected from a reference optical flat under it. Viewed in this manner, tiny areas of a surface are characterized by a pattern of fringes--an optical contour map quite similar to the geologists's topographic contours. The microstructures thus revealed are providing clues to puzzles in a whole host of disciplines--from crystal physics to metallurgy.

32. Arthur D. Little, Inc: Hydrogen Handbook, A compilation of Properties, Handling and Testing Procedures, Compatibility with Materials and Behavior at Low Temperatures. Under Contract with Parker Aircraft Co., AFFTC TR60-19, April 1960. Contract AF33(616)6710, AD 242285.

This report summarizes (1) experience with and the available technical information on the development of two prototype valves, one for a cryogenic gas service and the other for a cryogenic liquid service (these valves are under development by Parker Aircraft Co. for Government agency); (2) bibliographical information on the physical and mechanical properties of specific construction materials for temperature range of -420 to +200 F (these materials include some austenitic stainless steels and Teflon plastics); (3) the thermodynamic properties of helium, hydrogen, and nitrogen fluids with which the valves may be used or tested; (4) the hazards associated with the transportation and storage of hydrogen and with its use for testing two prototype valves for leakage across the seats; and (5) the sources and availability of hydrogen, and the Los Angeles regulations that apply to its transportation and use.

33. Whittaker Controls, Los Angeles, Calif.: The Physical and Thermodynamic Properties of Helium, September 1960.

This report briefly summarizes currently available information on the physical and thermodynamic properties of gaseous helium. The information is presented in both tabular and diagrammatic form to facilitate its use by design and test engineers who work with pressurized helium.

The reported property values for helium cover the pressure range of 14.7 to 6000 psia, and the temperature range of -44 to 600 F, with minor exceptions where data were limited or unavailable.

34. Stair, W. K.: Bibliography on Dynamic Shaft Seals, Preliminary Issue, University of Tennessee, Engineering Experiment Station, May 1962, 97 pages, 353 References.
35. King, A. L.: Bibliography on Fluid Sealing, BIB-1, British Hydrodynamics Research Association (B.H.R.A.) South Road, Temple Fields, Harlow, Essex, England, May 1962, 373 References.
36. General Electric Company: Study of Dynamic and Static Seals for Liquid Rocket Engines, NASA Contract No. NAS7-102, Final Report Vols. 1 and 2, 25 February 1963, 2164 References.

APPENDIX D

DISTRIBUTION LIST FOR FINAL REPORT

Contract NAS8-11325

"Investigation of Positive Type Shaft Seals"

INSTRUCTIONS

Report is to be sent directly to the "Recipient" marked with an "X" under the column headed "Designee" on pages 49 and 50 only. On pages 51 through 57, the report should be sent to the Technical Librarian of the "Recipient" with a carbon copy of the letter of transmittal to the attention of the person named under the column "Designee." The letter of transmittal should contain the contract number and complete title of the final report.

<u>Copies</u>	<u>Recipient</u>	<u>Designee</u>
1	NASA Headquarters, Washington, D.C. 20546	
1	Contracting Officer	()
1	Patent Office	()
	NASA Lewis Research Center	
	21000 Brookpark Rd., Cleveland, Ohio 44135	
1	Office of Technical Information	()
1	Contracting Officer	()
1	Patent Office	()
	NASA Manned Spacecraft Center	
	Houston, Texas 77001	
1	Office of Technical Information	()
1	Contracting Officer	()
1	Patent Office	()
	NASA Marshall Space Flight Center	
	Huntsville, Alabama 35812	
2	Office of Technical Information, A&TS-MS-IP	(X)
1	Technical Library, A&TS-MS-IL	(X)
1	Purchasing Office, A&TS-RP-MB	(X)
1	Patent Office, A&TS-M-PAT	(X)
1	Dale Burrows, S&E-ASTN-PJ	(X)
1	Technology Utilization Office, A&TS-MS-T	(X)
4	Forrest D. Pitsenberger, S&E-ASTN-EPB	(X)

<u>Copies</u>	<u>Recipient</u>	<u>Designee</u>
1	NASA Pasadena Office 4800 Oak Grove Drive, Pasadena, Calif. 91103 Patents and Contracts Management	()
3	Chief, Liquid Experimental Engineering, RPX or	(Not both)
3	Chief, Liquid Propulsion Technology, RPL Office of Advanced Research and Technology NASA Headquarters Washington, D.C. 20546	
1	Director, Technology Utilization Division Office of Technology Utilization NASA Headquarters Washington, D.C. 20546	
25	NASA Scientific and Technical Information Facility P.O. Box 33 College Park, Maryland 20740	
1	Director, Launch Vehicles and Propulsion, SV Office of Space Science and Applications NASA Headquarters, Washington, D.C. 20546	
1	Director, Advanced Manner Missions, MT Office of Manned Space Flight NASA Headquarters, Washington, D.C. 20546	
1	Mission Analysis Division NASA Ames Research Center Moffett Field, California 94035	

NASA FIELD CENTERS

<u>Copies</u>	<u>Recipient</u>	<u>Designee</u>
2	Ames Research Center Moffett Field, California 94035	Hans M. Mark
2	Goddard Space Flight Center Greenbelt, Maryland 20771	Merland L. Moseson Code 620
2	Jet Propulsion laboratory California Institute of Technology 4800 Oak Grove Drive Pasadena, California 91103	Henry Burlage, Jr. Propulsion Div., 38
2	Langley Research Center Langley Station Hampton, Virginia 23365	Ed Cartwright Director
2	Lewis Research Center 21000 Brookpark Road Cleveland, Ohio 44135	Dr. Abe Silverstein Director
2	Marshall Space Flight Center Huntsville, Alabama 35812	Hans G. Paul Code R-P&VED
2	Manned Spacecraft Center Houston, Texas 77001	Joseph G. Thibodaux Chief, Propulsion & Power Division
2	John F. Kennedy Space Center, NASA Cocoa Beach, Florida 32931	Dr. Kurt H. Debus

GOVERNMENT INSTALLATIONS

1	AFML (MANC) Wright-Patterson Air Force Base Dayton, Ohio 45433	D. L. Schmidt
1	Commander, Office of Research Analysis (OAR) Holloman Air Force Base, New Mexico 88330	Code RRRD
1	Air Force Missile Test Center Patrick Air Force Base, Florida	L. H. Ullian
1	Space and Missile Systems Organization Air Force Unit Post Office Los Angeles, California 90045	Col. Clark Technical Data Center

GOVERNMENT INSTALLATIONS (Continued)

<u>Copies</u>	<u>Recipient</u>	<u>Designee</u>
1	Arnold Engineering Development Center Arnold Air Force Station Tullahoma, Tennessee 37388	Dr. H. K. Doetsch
1	Bureau of Naval Weapons Department of the Navy Washington, D.C. 20546	J. Kay RTMS-41
1	Defense Documentation Center Headquarters Camerson Station, Building 5 5010 Duke Street Alexandria, Virginia 22314 Attn: TISIA	
1	Headquarters, U.S. Air Force Washington, D.C. 20546	Col. C. K. Stambaugh AFRST
1	Picatinny Arsenal Dover, New Jersey 07801	I. Forsten, Chief Liquid Propulsion Laboratory SMUPA-DL
1	Air Force Rocket Propulsion Laboratory Research and Technology Division Air Force Systems Command Edwards, California 93523	RPRR/Mr. H. Main
1	U.S. Army Missile Command Redstone Arsenal Alabama 35809	Mr. Walter Wharton
1	U.S. Naval Weapons Center China Lake, California 93557	Code 4562 Chief, Missile Propulsion Division
<u>C P I A</u>		
1	Chemical Propulsion Information Agency Applied Physics Laboratory 8621 Georgia Avenue Silver Spring, Maryland 20910	Tom Reedy

INDUSTRY CONTRACTORS

<u>Copies</u>	<u>Recipient</u>	<u>Designee</u>
1	Aerojet-General Corporation P.O. Box 296 Azusa, California 91703	W. L. Rogers
1	Aerojet-General Corporation P.O. Box 1947 Technical Library Bldg. 2015, Dept. 2410 Sacramento, California 95803	R. Stiff
1	Space Division Aerojet-General Corporation 9200 East Flair Drive El Monte, California 91734	S. Machlawski
1	Aerospace Corporation 2400 East El Segundo Boulevard P.O. Box 95085 Los Angeles, California 90045	John G. Wilder MS-2293
1	Astrosystems International, Inc. 1275 Bloomfield Avenue Fairfield, new Jersey 07007	A. Mendenhall
1	Atlantic Research Corporation Edsall Road and Shirley Highway Alexandria, Virginia 22314	Dr. Ray Friedman
1	AVCO Systems Division Wilmington, Massachusetts	Howard B. Winkler
1	Beech Aircraft Corporation Boulder Division Box 631 Boulder, Colorado	J. H. Rodgers
1	Bell Aerosystems Company P.O. Box 1 Buffalo, New York 14240	W. M. Smith
1	Bellcomm 955 L'Enfant Plaza, S.W. Washington, D.C.	H. S. Lendon

INDUSTRY CONTRACTORS (Continued)

<u>Copies</u>	<u>Recipient</u>	<u>Designee</u>
1	Bendix Systems Division Bendix Corporation 3300 Plymouth Street Ann Arbor, Michigan	John M. Brueger
2	Boeing Company P.O. Box 3707 Seattle, Washington 98124	(1) J. D. Alexander (1) James Koh
1	Boeing Company 1625 K Street, N. W. Washington, D.C. 20006	Library
1	Boeing Company P.O. Box 1680 Huntsville, Alabama 35801	Ted Snow
1	Missile Division Chrysler Corporation P.O. Box 2628 Detroit, Michigan 48231	John Gates
1	Wright Aeronautical Division Curtiss-Wright Corporation Wood-Ridge, New Jersey 07075	G. Kelly
1	Research Center Fairchild Hiller Corporation Germantown, Maryland	Ralph Hall
1	Republic Aviation Corporation Fairchild Hiller Corporation Farmingdale, Long Island, New York	Library
1	General Dynamics, Convair Division Library & Information Services (128-00) P.O. Box 1128 San Diego, California 92112	Frank Dore
1	Missile and Space Systems Center General Electric Company Valley Forge Space Technology Center P.O. Box 8555 Philadelphia, Pa.	F. Mezger F. E. Schultz
1	Grumman Aircraft Engineering Corp. Bethpage, Long Island, New York	Joseph Gavin

INDUSTRY CONTRACTORS (Continued)

<u>Copies</u>	<u>Recipient</u>	<u>Designee</u>
1	Honeywell, Inc. Aerospace Division 2600 Ridgway Road Minneapolis, Minnesota	Gordon Harms
1	Hughes Aircraft Co. Aerospace Group Centinela and Teale Streets	E. N. Meier V.P. and Div. Mgr. Research and Dev. Division
1	Walter Kidde and Company, Inc. Aerospace Operations 567 Main Street Belleville, New Jersey	R. J. Hanville Director of Research Engineering
1	Ling-Temco-Vought Corporation P.O. Box 5907 Dallas, Texas 75222	Warren G. Trent
1	Arthur D. Little, Inc. 20 Acorn Park Cambridge, Massachusetts 02140	Library
1	Lockheed Missiles and Space Co. Attn: Technical Information Center P.O. Box 504 Sunnyvale, California 94088	J. Guill
1	Lockheed Propulsion Company P.O. Box 111 Redlands, California 92374	H. L. Thackwell
1	The Marquardt Corporation 16555 Saticoy Street Van Nuys, California 91409	Howard McFarland
1	Baltimore Division Martin Marietta Corporation Baltimore, Maryland 21203	John Calathes (3214)
1	Denver Division Martin Marietta Corporation P.O. Box 179 Denver, Colorado 80201	Dr. Morganthaler
1	Orlando Division Martin Marietta Corp. Box 5837 Orlando, Florida	J. Ferm

INDUSTRY CONTRACTORS (Continued)

<u>Copies</u>	<u>Recipient</u>	<u>Designee</u>
1	Astropower Laboratory McDonnell-Douglas Aircraft Company 2121 Paularino Newport Beach, California 92663	Dr. George Moc Director, Research
1	McDonnell Douglas Aircraft Corp. P.O. Box 516 Municipal Airport St. Louis, Missouri 63166	R. A. Herzmark
1	Missile and Space Systems Division McDonnell-Douglas Aircraft Company 3000 Ocean Park Boulevard Santa Monica, California 90406	R. W. Hallet Chief Engineer. Adv. Space Tech.
1	Space & Information Systems Division North American Rockwell 12214 Lakewood Boulevard Downey, California 90241	Library
1	Northrop Space Laboratories 3401 West Broadway Hawthorne, California	Dr. William Howard
	Aeronutronic Division Philco Corporation Ford Road Newport Beach, California 92663	D. A. Garrison
	Astro-Electronics Division Radio Corporation of America Princeton, New Jersey 08540	Y. Brill
	Rocket Research Corporation 11441 Willow Road Redmond, Washington 98052	Technical Library
	Sunstrand Aviation 2421 11th Street Rockford, Illinois 61101	R. W. Reynolds
	Stanford Research Institute 333 Ravenswood Avenue Menlo Park, California 94025	Dr. Gerald Marksman

INDUSTRY CONTRACTORS (Continued)

<u>Copies</u>	<u>Recipient</u>	<u>Designee</u>
1	TRW Systems Group TRW Incorporated One Space Park Redondo Beach, California 90278	G. W. Elverum
1	TAPCO Division TRW, Incorporated 23555 Euclid Avenue Cleveland, Ohio 44117	P. T. Angell
1	Thiokol Chemical Corporation Huntsville Division Huntsville, Alabama	John Goodloe
1	Research Laboratories United Aircraft Corporation 400 Main Street East Hartford, Connecticut 06108	Erle Martin
1	Hamilton Standard Division United Aircraft Corporation Windsor Locks, Connecticut 06096	R. Hatch
1	United Technology Center 587 Methilda Avenue P.O. Box 358 Sunnyvale, California 94088	Dr. David Altman
1	Florida Research and Development Pratt and Whitney Aircraft United Aircraft Corporation P.O. Box 2691 West Palm Beach, Florida 33402	R. J. Coar
1	Vickers, Inc. Box 302 Troy, Michigan	

UNCLASSIFIED

Security Classification

DOCUMENT CONTROL DATA - R & D

(Security classification of title, body of abstract and indexing annotation must be entered when the overall report is classified)

1. ORIGINATING ACTIVITY (Corporate author)

Rocketdyne, a Division of North American Rockwell Corporation, 6633 Canoga Avenue, Canoga Park, California 91304

2a. REPORT SECURITY CLASSIFICATION

UNCLASSIFIED

2b. GROUP

3. REPORT TITLE

FINAL REPORT, INVESTIGATION OF POSITIVE TYPE SHAFT SEALS

4. DESCRIPTIVE NOTES (Type of report and inclusive dates)

Final Report

5. AUTHOR(S) (First name, middle initial, last name)

Rocketdyne Engineering

6. REPORT DATE

14 November 1969

7a. TOTAL NO. OF PAGES

66

7b. NO. OF REFS

5

8a. CONTRACT OR GRANT NO.

NAS8-11325

b. PROJECT NO.

c.

d.

9a. ORIGINATOR'S REPORT NUMBER(S)

R-7986

9b. OTHER REPORT NO(S) (Any other numbers that may be assigned this report)

10. DISTRIBUTION STATEMENT

11. SUPPLEMENTARY NOTES

12. SPONSORING MILITARY ACTIVITY

13. ABSTRACT

The effect on seal leakage of surface finish, face load, leakage pressure, temperature, and sealed fluid were investigated. The fluids were gaseous helium, liquid hydrogen, and water. Results of a test program conducted for the investigation are presented, and a literature survey is included.

14. KEY WORDS	LINK A		LINK B		LINK C	
	ROLE	WT	ROLE	WT	ROLE	WT
Surface Finish						
Face Load						
Leakage Pressure						
Temperature						
Sealed Fluid						
Gaseous Helium						
Liquid Hydrogen						
Water						
Seal Tester Design						
Test Procedure and Apparatus						
Instrumentation						
Leakage Flow Analysis						
Flow Theory						
Flow Regime Method						
Literature Survey						

